Available online at www.sciencedirect.com
ScienceDirect
Acta Materialia 57 (2009) 3497–3508
Acta MATERIALIA
www.elsevier.com/locate/actamat

Onset of sidewise instability and cell–dendrite transition in directional solidification

J. Teng [a,b], S. Liu [a,c], R. Trivedi [a,*]

[a] Materials Sciences, Ames Laboratory-USDO and Department of Materials Science and Engineering, Iowa State University, Ames, IA 50011, USA
[b] SSCI An Aptuit Company, West Lafayette, IN 47906, USA
[c] General Electric Co., Greenville, SC 29615, USA

Received 29 October 2008; received in revised form 2 April 2009; accepted 5 April 2009
Available online 18 May 2009

Abstract

The transition from cellular to dendritic microstructure in directional solidification is investigated in succinonitrile (SCN)–camphor alloys. This transition is found not to be sharp, but occurs locally over a range of velocities or thermal gradients, and the diffuseness of the transition is related to the existence of a range of primary spacing. Within the transition zone, critical cell spacing λ_{cd} is present where a cell just develops sidewise perturbations. An expression for the critical spacing for the onset of sidewise perturbation is obtained, and it is used to establish the conditions for the start and end of the transition. The results of the present study are then synthesized with those in the SCN–acetone system to incorporate the effect of system parameters on the onset of sidewise instability.

Keywords: Directional solidification; Solidification microstructure; Cellular growth; Dendritic growth; Interface dynamics

1. Introduction

Transitions from a planar to a non-planar interface at a low velocity and that from a non-planar to a planar interface at a high velocity have been well established, and these transitions have been shown to be sharp, so that they can be described by specific relationships between the velocity V, thermal gradient G and alloy composition C_0 [1]. In contrast, the transition from cellular to dendritic microstructure at low velocity and the reverse transition from dendritic to cellular interface at high velocity have not been accurately characterized. Early attempts assumed the transitions to be sharp, and proposed criteria for cell to dendrite transition in terms of experimental variables G, V and C_0 [2–6]. Tewari and Laxmanan [7] compared all the published experimental results with different theoretical models based on the sharp transition, and concluded that no model could explain all the experimental results.

Important progress on the cell–dendrite transition (CDT) was made by Georgelin and Pocheau [8] and Trivedi et al. [9], who quantitatively characterized the conditions for the onset of sidewise instabilities in thin samples of transparent materials in which dynamics of the transition can be visualized in situ and the growth is controlled by solute diffusion. They observed that the process of side-branch initiation is not a collective behavior for normal array growth; rather, it occurs locally such that a specific cell in a given array develops side-branch instabilities when its local primary spacing exceeds some critical value. This is due to the presence of a range of cell spacing in a given array, and the CDT occurs over a range of experimental conditions (V, G and C_0). Here, the term dendrite is used as a primary arm in which sidewise instabilities are observable within the optical resolution. The start of the transition is considered when the largest cell spacing in an array just exhibits sidewise instability, and the transition is complete when the smallest cell spacing in the array forms side branches, so that all cells in an array have transformed into dendrites. Within the transition zone, the sidewise

* Corresponding author.
E-mail address: trivedi@ameslab.gov (R. Trivedi).

1359-6454/$36.00 © 2009 Acta Materialia Inc. Published by Elsevier Ltd. All rights reserved.
doi:10.1016/j.actamat.2009.04.005

instability occurs when the local spacing approaches a critical value λ_{cd}, which is related to the growth parameters. Limited experimental studies in the literature on the effect of composition, growth rate and thermal gradient on the critical spacing have not been consistent [8,9]. This is because the critical spacing is very sensitive to the experimental design, and several conditions, described in the experimental section, must be satisfied to obtain unambiguous results.

The major objectives of the present study are as follows: (1) to characterize quantitatively the relationship between the critical spacing and experimental parameters (G, V, C_0) in well-characterized experiments in the succinonitrile (SCN)–camphor system; the critical spacing is found to be described by the relationship: $\lambda_{cd} = A(D\Gamma)^{1/3}(GV)^{-1/3}C_0^{-1/4}$, where D is the diffusion coefficient in the liquid, Γ is the Gibbs–Thomson coefficient, and A is a constant that depends on the system parameters; (2) to validate the above result by analyzing the existing data in the SCN–acetone system, and obtain an expression for the constant A in terms of system parameters; (3) to obtain the conditions for the start and end of the transition that depends on G, V and C_0; (4) to establish quantitatively the characteristics of cells and dendrites within the coexistence region, which are different from those in a purely cellular or purely dendritic array, through the measurements of the primary and initial secondary arm spacing, tip radius and tip shape.

2. Experimental

SCN–camphor alloys were selected for this study because the dynamics of pattern formation can be observed in situ, and the phase diagram and relevant thermo-physical properties of this system have been determined accurately [10,11]. A temperature gradient stage (TGS) was used for the directional solidification process. The sample was moved through a linear translation system driven by a computer-modulated step motor. The temperature gradient (G) was varied by adjusting the gap between the hot and cold blocks and/or adjusting the temperature settings. The TGS was mounted on the stage of an optical microscope, and the interface patterns were monitored through an imaging system and recorded by a high-resolution digital camera. The whole set-up was placed inside a glove box with feedthroughs for electrical connections, heating and cooling fluids and dry N_2, to minimize fluctuations of the hot block temperature. The stability of the hot zone temperature was examined in one experiment by monitoring its temperature over 1404 s. A random variation in the temperature was observed, with a statistical distribution showing a normal distribution with the mean 67.525 °C and the standard deviation (σ) 0.039 °C. Furthermore, actual temperature profiles were obtained for each run, and the thermal gradient was determined from the linear regression of the data near the interface temperature to obtain the temperature gradient values.

The inside dimensions of the rectangular sample were length 300 mm, width 4.0 mm and thickness 0.2 mm. Owing to the limited width of the sample, dummy glass tubes of the same dimensions were placed on each side of the sample to minimize the lateral heat flow. The three-tube configuration was sandwiched between two glass plates to stabilize the thermal profile in the sample.

Because the CDT is sensitive to several experimental design parameters, the following aspects of the experimental design must be considered to obtain reliable results.

First, both the components of the alloy must be stable under experimental conditions. Consequently, the hot zone temperature was kept <120 °C to avoid disintegration of SCN, and camphor was found to be stable in the system at the hot zone temperature.

Secondly, both components must be purified to remove impurities that significantly influence the conditions for the transition. As-received SCN contains several impurities [12] which must be removed first. SCN was purified by distillation under vacuum and multi-stage zone refining. Camphor was purified by sublimation under vacuum. To

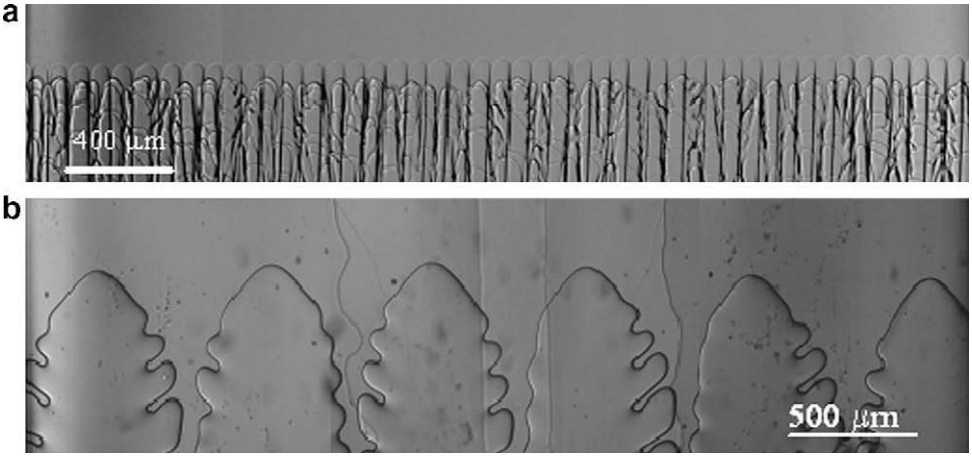

Fig. 1. Interface morphology of (a) SCN–0.035 wt.% camphor ($G = 1.36$ K mm^{-1}, $V = 21.2$ μm s^{-1}) and (b) SCN–0.65 wt.% camphor ($G = 1.36$ K mm^{-1}, $V = 0.51$ μm s^{-1}) in a 200-μm-thick sample.